

RESEARCH ARTICLE

 OPEN ACCESS

Comparing Modes of Transmission for Sarcoptic Mange Dynamics and Management in Bare-Nosed Wombats

Nicholas J. Beeton,^{a,b,c} Lawrence K. Forbes,^b Scott Carver^c^aCSIRO, 3 Castray Esplanade, Battery Point TAS 7004, Australia; ^bDiscipline of Mathematics and Physics, University of Tasmania, Australia; ^cDiscipline of Biological Sciences, University of Tasmania, Australia**ABSTRACT**

How hosts become exposed to environmentally transmitted pathogens has significant consequences for their dynamics and control, including conservation-critical cases. We investigate whether dynamics of the globally important parasite *Sarcoptes scabiei* are strongly influenced by transmission. We compare two transmission models, based on mange transmission in the bare-nosed wombat *Vombatus ursinus*: a published model of exposure via free mixing in the environment, and a novel spatially implicit model representing binary exposure. We also integrate disease management into our models. We confirm up to four steady states are possible in either model, demonstrating that robust mathematical conclusions underpin previous empirical observations. We present detailed analytical and numerical evidence that a disease-free steady state is achievable for wombats under a range of treatment strategies, though more treatment effort is required in the case of binary exposure. These results enhance confidence in the success of applied management of environmentally transmitted pathogens impacting wildlife.

ARTICLE HISTORYReceived July 16, 2020
Accepted January 27, 2021**KEYWORDS**

wildlife disease, dynamical systems analysis, Susceptible-Exposed-Infectious-Recovered, environmental transmission

1 Introduction

Pathogens that are transmitted between hosts via the environment are responsible for some of the most conservation-critical diseases facing wildlife (e.g., Bat White Nose syndrome, chytridiomycosis, Chronic Wasting Disease, sarcoptic mange) (Tompkins et al., 2015). The development of theory relating to environmentally transmitted pathogens is therefore of direct relevance to contemporary conservation issues, including the properties governing disease dynamics and assessment of disease-management strategies. For example, the nature of host exposure to pathogen fomites in the environment (e.g., whether exposure is characterised as generalised, binary, density- or frequency-dependent) can have consequences for thresholds of pathogen-driven host declines, host-pathogen coexistence, and pathogen extinction (Devenish-Nelson et al., 2014; Beeton et al., 2019). Understanding how the nature of pathogen exposure influences host-pathogen thresholds can influence the effectiveness of disease-mitigation strategies (Joseph et al., 2013). Thus, theoretical studies interrogating environmentally transmitted pathogens of wildlife based on empirical foundations are of both specific and general value.

Among the most generalist of mammalian pathogens is the parasitic mite *Sarcoptes scabiei*, which causes the disease scabies (in humans) or sarcoptic mange (in other animals) (Fraser et al., 2016). Depending on host species, *S. scabiei* can be environmentally or directly transmitted (Arlian and Morgan, 2017). It has been documented to affect wildlife populations, including canids (e.g., *Vulpes vulpes*, *Vulpes macrotis*, *Canis lupus*, *Nycterautes procyonoides*), felids (e.g., *Acinonyx jubatus*, *Panthera leo*), ungulates (e.g., *Syncerus caffer*, *Capra ibex*, *Capricornis swinoei*), primates (e.g., *Gorilla gorilla*, *Pan paniscus*) and marsupials (e.g., *Vombatus ursinus*, *Phascolarctos cinereus*) (Bornstein et al., 2001; Pence and Ueckermann, 2002; Astorga et al., 2018). Scabies is also among the 30 most prevalent human pathogens and was recently declared by the World Health Organisation as a Neglected Tropical Disease (Mounsey et al., 2016). A range of disease dynamic patterns are observed for *S. scabiei* in wildlife populations, including stable coexistence, limit cycles and extirpation of host and pathogens (Beeton et al., 2019). Additionally, *S. scabiei* is subject to various intervention strategies in both human and non-human populations using a range of parasiticides, delivered in a variety of ways dependent on whether the specific host-parasite transmission is direct or environmental (Arlian and Morgan, 2017).

The bare-nosed wombat (*Vombatus ursinus*, a.k.a. common wombat) is the wildlife species most affected by sarcoptic mange

in Australia (Fraser et al., 2016). Owing to the solitary nature of bare-nosed wombats (hereafter referred to as ‘wombats’) transmission between individuals is overwhelmingly through environmental fomites (Skerratt et al., 1999; Skerratt, 2005; Martin et al., 2018). There is much uncertainty around the nature of their environmental exposure to *S. scabiei*, owing to challenges associated with sampling mites from the environment. The general assumption is that transmission occurs in burrows, which these nocturnal marsupials reside in during the day, although this has never been directly tested. There are multiple dynamic scenarios observed for wombats and mange disease. Empirical research has shown population extirpation, coexistence and pathogen fade-out resulting in disease-free equilibria for wombats and *S. scabiei* (Martin et al., 2018). These observations are supported by theoretical models (Beeton et al., 2019). In addition, there is much applied management and public interest in controlling mange disease in wombat populations due to *S. scabiei* being an invasive parasite to Australia, introduced by European settlers and their domestic animals (Fraser et al., 2016).

The manner in which susceptible wombats become exposed to *S. scabiei* may have important implications for understanding empirical disease dynamics and disease mitigation strategies, and this is not well understood. In one scenario, as modelled in Beeton et al. (2019), wombats experience generalised exposure to mange-causing mites via the environment, consistent with a population that is mixing relatively freely in the environment where pathogen fomites exist. This type of mixing is common to many mechanistic models that accurately capture empirical disease and host-population dynamics, even though population mixing is almost always more heterogeneous (Keeling and Rohani, 2008). Indeed, much contemporary research has focused on understanding the role of heterogeneities (i.e., contact and transmission heterogeneity) on disease and population dynamics (Lloyd-Smith et al., 2005). For wombats, evidence suggests that they are primarily exposed in the bedding chambers of burrows in which they sleep (Skerratt, 2005). As wombats periodically switch the burrow in which they sleep (Martin et al., 2018), exposure of susceptible individuals may therefore be binary in nature (i.e., the burrow either contains mites which wombats get exposed to, or not), rather than a freely mixing scenario. Modelling this heterogeneity in transmission among wombat burrows requires a qualitatively different approach; we adopt a spatially implicit approach for simplicity (Lopes et al., 2010), as opposed to opting for a spatially explicit approach using metapopulations (Snäll et al., 2008) or individual-based models.

In this present study, we ask to what extent is mechanistic modelling that treats transmission of *S. scabiei* among wombats as free mixing robust to the other extreme of transmission, binary exposure in burrows? This question is of both fundamental and applied value, as the extent of congruence has implications for the dynamical properties of the system, disease-control programs aimed at mite eradication to protect bare-nosed wombats against disease-driven population declines, and even local extinction events.

We may not necessarily be able to expect even qualitatively similar results after changing the model structure: such changes can cause unpredictable results due to emergent behaviour in nonlinear systems, and many canonical examples exist demonstrating this. The discrete logistic map is used to model populations with non-overlapping generations, yet can lead to chaos under certain parameter values, despite such behaviour being entirely absent from its continuous-time analogue (May, 1976). The Lotka-Volterra system used to model competing species converges to a stable equilibrium for two species, but is capable of a wide range of behaviours for three or more (May, 1976). Systems that are locally stable can become unstable when made spatially explicit and diffusion is introduced, potentially leading to Turing patterns (Turing, 1952).

2 The Mathematical Model

We consider a total population of $N(t)$ wombats, and we suppose that there are four sub-populations, with $S(t)$, $E(t)$, $I(t)$ and $R(t)$ individuals in each. The symbol t denotes time measured in days, and we clearly have

$$N = S + E + I + R. \quad (1)$$

These four sub-populations S , E , I and R correspond approximately to the usual four sub-groups Susceptible, Exposed, Infected and Recovered (Beeton et al., 2019), familiar from classical disease-spread models. Here, $S(t)$ are the susceptible wombats, and the ‘‘exposed’’ class $E(t)$ represents wombats carrying a few mites, but are not yet showing symptoms of mange. We adopted an E and I class in our models as they reflect the conditions observable in the field. Early stages of *S. scabiei* infection are inapparent in wombats and generally not possible to diagnose relative to healthy individuals. However, as infection increases, signs of disease develop and are diagnosable both clinically and by observation (Fraser et al., 2018; Martin et al., 2019). The infected group $I(t)$ are those with significant mite infestation who are sick or enfeebled as a result. Finally, there are the ‘‘recovered’’ individuals $R(t)$ that are resistant to mite infestation, at least in the short term, following treatment for the mites.

Wombats spend a significant fraction of their time living in underground burrows. While wombats are solitary, they do share the same burrows in which they sleep asynchronously, owing to switching burrows periodically (around once per week) (Martin et al., 2019). Thus, although the mites do not survive long by themselves outside of the burrow (up to around 19 days), they may be transmitted from one wombat to another through the material in the burrow bedding chamber, in a type of second-order contact process. To avoid the added complexity of a spatially explicit approach, we instead opt for a spatially implicit

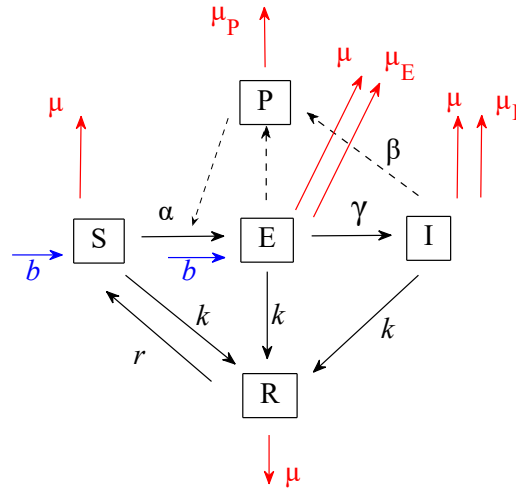


Figure 1: Schematic diagram of the interaction between wombat sub-populations. The probability P of wombat infection through an infected burrow is also indicated on the diagram, and its effective interaction with the population groups is indicated with dashed lines. (For interpretation of the references to colour in this figure legend, the reader is referred to the web version of this article.)

approach (e.g., see Lopes et al., 2010). We achieve this by using a fifth variable $P(t)$, which is the proportion of burrows that contain enough mites to ensure infection of any wombat that enters them. Clearly $0 \leq P \leq 1$, and so $P(t)$ also represents the probability of infection of a wombat entering a new burrow at random. This situation is illustrated in Figure 1. The second-order term αSP thus gives the rate at which susceptible individuals are immediately transformed into “exposed” ones, with parameter α representing a constant rate of movement of susceptible wombats between burrows at random. Exposed wombats then become infected at a constant rate γ . The constant μ is the natural death rate of all wombats, and the additional constants μ_E and μ_I are the extra rates at which the exposed and the infected individuals E and I die as a result of the mites they carry. We note that the rate of transition of wombats from E to I is twice as high as μ_E (see Section 5), and thus has negligible influence on interpretation of the models. The natural mortality rate of the mites is responsible for the constant μ_P , the rate at which burrows lose their infectious status. Wombats can be treated for mange using various pesticides, distributed indiscriminately at a population scale, making them temporarily resistant to infection (Martin et al., 2019). Once a wombat becomes resistant to the mites, the constant r in Figure 1 corresponds to the reversion rate at which the treatment wears off and recovered wombats become susceptible. To protect or treat the wombats, field ecologists are experimenting with small flaps, laced with parasiticides, placed over the entries to their burrows, and which the wombats must contact each time they enter or leave the burrow (Martin et al., 2019). This provides a constant rate k at which wombats become resistant.

A logistic birth rate for wombats is assumed, and the population of wombats is made dimensionless by scaling it against the carrying capacity of the environment. Consequently, the dimensionless fecundity-limiting capacity is 1, and the overall population increase rate behaves like $bN(1 - N)$ for some constant birth rate b per wombat. The function $N(t)$ is the total wombat population in (1).

These modelling assumptions, combined with Figure 1, may be developed into a series of ordinary differential equations (ODEs) for each of the five variables that describe this system. The rate of increase in the Susceptible sub-population is

$$\frac{dS}{dt} = [bN(1 - N) + rR](1 - P) - \alpha SP - (\mu + k)S, \quad (2)$$

and the “exposed” population varies as

$$\frac{dE}{dt} = [bN(1 - N) + rR + \alpha S]P - (\mu + \gamma + k + \mu_E)E. \quad (3)$$

Since this model assumes that mite infection occurs only in the wombat burrows, where also new wombats are born, both the susceptible S and exposed E populations contain the logistic birth term. Wombats are born susceptible if their burrow does not contain mites, and the probability of this is $(1 - P)$. On the other hand, wombats are exposed at birth if they are born to a mother in a mite-laden burrow, and the proportion of these is P .

From Figure 1, the number of infected wombats changes according to the rate law

$$\frac{dI}{dt} = \gamma E - (\mu + k + \mu_I)I \quad (4)$$

and the population of resistant wombats changes as

$$\frac{dR}{dt} = k(S + E + I) - (\mu + r)R. \quad (5)$$

It is also necessary to account for the changing proportion P of infected burrows, and from Figure 1,

$$\frac{dP}{dt} = \beta(E + I)(1 - P) - \mu_P P. \quad (6)$$

In equation (6), the first term indicates that the rate of increase of infected burrows is proportional to the number of uninfected burrows that are occupied by either an exposed E or an infected wombat I , multiplied by a burrow infection rate β . The term $-\mu_P P$ provides a mechanism for an infected burrow to become uninfected once again, as the mites within it die at a rate μ_P .

Note that this rate depends on infectious wombats remaining in the burrow and regularly shedding mites rather than just visiting it, as for wombat infection. To illustrate, assume that there are B available burrows and denote $F = BP$ as the number of infectious burrows with a high fomite load. Then

$$\frac{dF}{dt} = \xi(E + I)\frac{B - F}{B} - \mu_P F,$$

assuming that wombats are randomly dispersed among burrows and that uninfected burrows containing an infected wombat will become infectious at some rate ξ . Then

$$\frac{dP}{dt} = \frac{1}{B} \frac{dF}{dt} = \frac{\xi}{B}(E + I)(1 - P) - \mu_P P$$

so the burrow infection rate $\beta = \xi/B$ is the infection rate of an individual burrow divided by the total number of burrows.

For the purposes of direct comparison, we show the equations from Beeton et al. (2019) with their equivalents in equations (1)–(6), where these differ. The equations for $\frac{dI}{dt}$ and $\frac{dR}{dt}$ are identical for both models.

$$\begin{aligned} \frac{dS}{dt} &= \begin{cases} bN(1 - N) + rR - \frac{\beta SF}{1 + F} - (\mu + k)S, & \text{from Beeton et al., 2019} \\ [bN(1 - N) + rR](1 - P) - \alpha SP - (\mu + k)S & \text{from eq. (2)} \end{cases} \\ \frac{dE}{dt} &= \begin{cases} \frac{\beta SF}{1 + F} - (\mu + \gamma + k + \mu_E)E, & \text{from Beeton et al., 2019} \\ [bN(1 - N) + rR + \alpha S]P - (\mu + \gamma + k + \mu_E)E & \text{from eq. (3)} \end{cases} \\ \frac{dF}{dt} &= f(E + I) - \mu_F F & \text{from Beeton et al., 2019} \\ \frac{dP}{dt} &= \beta(E + I)(1 - P) - \mu_P P & \text{from eq. (6)} \end{aligned}$$

The major aim of this present paper is to determine the extent to which this new model, described by equations (1)–(6), gives predictions that are compatible with those of the previous description of wombat-mite interaction. This will be an important indicator of how robust such models are in their ability to provide consistent management strategies.

While the two models describe the same system, the mechanisms are quite different. In the previous work, all susceptible wombats are assumed to be equally susceptible to infection and thus enter the exposed class at the same rate. The current work differs in two respects: susceptible wombats *cannot* be infected until they enter an infected burrow, at which point they *will be* infected. In other words: in the previous work heterogeneities in the environment had no effect on the model, but here the infection status of wombats is entirely dependent on their local environment in a binary sense, with their movement through the environment being the determining factor. In this respect, it more closely represents reality in the field.

This comparison is important, since if the two are in broad agreement, then the results are more robust and are therefore likely to be seen in actual field studies. This would then indicate that the mite eradication schemes these models suggest are likely to be effective in protecting bare-nosed wombats against severe loss and even possible extinction, as a result of sarcoptic mange. Any differences in the two models may also point to potential unforeseen outcomes due to model assumptions that can then be accounted for.

3 Steady State Populations

Our previous study (Beeton et al., 2019) of sarcoptic mange in wombats identified four different steady states. The first resulted in complete extinction of both mites and wombats, and there was a second state in which the wombats survived but the mites did not. This second state would be the aim of any treatment regime against sarcoptic mange. There were also two further endemic states in which both mites and wombats survived, although one of these states contained some negative sub-populations and so is not a biologically meaningful outcome.

The present model likewise contains four steady states. There is again a state of total extinction, in which all the sub-populations are zero and the proportion of infected burrows is also therefore zero. Mathematically,

$$(S_{eq}, E_{eq}, I_{eq}, R_{eq}, P_{eq}) = (0, 0, 0, 0, 0). \quad (7)$$

Disease-spread models commonly contain such an extinction state, as discussed by Hethcote (2000).

There is also a steady state solution in this model, in which wombats survive but mites do not, as in Beeton et al. (2019). We follow that paper and define constants

$$\begin{aligned} \lambda_0 &= \mu + r \\ \lambda_R &= \mu + r + k, \end{aligned} \quad (8)$$

so that the second equilibrium can be written succinctly as

$$(S_{eq}, E_{eq}, I_{eq}, R_{eq}, P_{eq}) = \left(\frac{\lambda_0(b - \mu)}{b\lambda_R}, 0, 0, \frac{k(b - \mu)}{b\lambda_R}, 0 \right). \quad (9)$$

The total mite population in (1) in this case becomes simply $N_{eq} = (b - \mu)/b$. This is identical to their mite-free equilibrium.

As with the previous model, there are two further endemic steady states in this new model. It is convenient to define additional constants

$$\begin{aligned} m_I &= \mu + k + \mu_I \\ m_E &= \mu + k + \mu_E \\ m_A &= \mu + k + \alpha. \end{aligned} \quad (10)$$

Then it follows from (4) and (5) that the equilibrium populations are related according to

$$\begin{aligned} E_{eq} &= \frac{m_I}{\gamma} I_{eq} \\ S_{eq} &= \frac{\lambda_0}{k} R_{eq} - \frac{(m_I + \gamma)}{\gamma} I_{eq}, \end{aligned} \quad (11)$$

making use of the constants defined in (8). The steady-state distribution of infected burrows is found from (6) to be

$$P_{eq} = \frac{\beta(m_I + \gamma)I_{eq}}{\gamma\mu_P + \beta(m_I + \gamma)I_{eq}}, \quad (12)$$

in terms of the equilibrium number I_{eq} of infected wombats. So long as $I_{eq} \geq 0$, the proportion of infected burrows in (12) lies in the interval $0 \leq P_{eq} \leq 1$, as required. It follows from (1) that the total wombat population at equilibrium has the simple form $N_{eq} = (\lambda_R/k)R_{eq}$.

To derive expressions for the endemic populations, it is useful to define further constants

$$\begin{aligned} \phi &= \frac{\alpha}{\beta} \mu_P m_I (m_E + \gamma) \\ \psi &= \frac{\alpha}{\gamma} (m_I + \gamma) [\alpha(m_I + \gamma) + m_I(m_E + \gamma)] \\ \sigma &= b\lambda_R + kr + \alpha\lambda_0, \end{aligned} \quad (13)$$

where use has been made of the constants (8) and (10). Then the steady-state form of (3) shows that

$$I_{eq} = \frac{\alpha(m_I + \gamma)}{\psi} \left[\frac{\sigma}{k} R_{eq} - b \left(\frac{\lambda_R}{k} \right)^2 R_{eq}^2 \right] - \frac{\phi}{\psi}. \quad (14)$$

Finally, it remains to derive an equation for R_{eq} from which all the other equilibrium quantities can then be calculated. The steady-state forms of (2) and (3) are added, and use is made of the expressions (11), (12) and (14) to give, after some algebra, the quadratic equation

$$0 = b\alpha m_A \left(\frac{\lambda_R}{k}\right)^2 (m_I + \gamma)^2 R_{eq}^2 - \alpha \tilde{P} \left(\frac{\lambda_R}{k}\right) (m_I + \gamma) R_{eq} - \phi \tilde{Q}. \quad (15)$$

Here, the additional constants

$$\begin{aligned} \tilde{Q} &= \mu_E m_I + \mu_I \gamma \\ \tilde{P} &= (b - \mu) [\alpha (m_I + \gamma) + m_I (m_E + \gamma)] - \frac{\sigma}{\lambda_R} \tilde{Q} \end{aligned} \quad (16)$$

have been defined for convenience. This quadratic equation (15) has much in common with the equation in Beeton et al. (2019) for the endemic states in that model. Its two solutions are

$$R_{eq} = \frac{k}{2b\alpha m_A \lambda_R (m_I + \gamma)} \left[\alpha \tilde{P} \pm \sqrt{(\alpha \tilde{P})^2 + 4b\alpha m_A \phi \tilde{Q}} \right]. \quad (17)$$

The constants ϕ defined in (13) and \tilde{Q} in (16) are both positive, and so it follows from the solution (17) that both values of R_{eq} are real, with the positive sign giving a positive value for R_{eq} and the negative sign giving a negative value. The equilibrium obtained with the negative sign in (17) is therefore never of any biological significance. The other endemic state, with the positive sign, always gives $R_{eq} > 0$ but may nevertheless give some negative values for the other equilibrium populations in (11), (12) and (14), depending on the values of the constants in the model. In those cases, this second endemic steady state is also not biologically meaningful, in which case only the extinction state (7) and the no-mites state (9) would remain. This situation may even be optimal, in a biological sense, since it is the mite-free equilibrium (9) that is the most desirable from the point of view of protecting bare-nosed wombats.

4 Stability of Equilibria

We are concerned to know the conditions under which the mite-free steady state (9) is stable, since to achieve this state in the field would be the aim of any treatment programme.

For the total extinction steady state (7) in Section 3, the eigenvalues may be determined as the roots of the characteristic equation $\det(\mathbf{J} - \Lambda \mathbf{I}) = 0$, and after some algebra are found to be

$$\Lambda = -\mu_P; \quad -(\gamma + m_E); \quad -m_I; \quad -\lambda_R; \quad (b - \mu) \quad (18)$$

The first four of these are negative, but the last one is positive in our case of interest $b > \mu$, where we define the wombat birth rate b to exceed the death rate by natural causes μ . In the converse case $b < \mu$, all eigenvalues are negative, meaning the wombat population will always become extinct even in the absence of mites, which is not of interest to us from a dynamics perspective. This is therefore an unstable equilibrium, behaving as a saddle in 5-dimensional phase space. This dynamical behaviour near the total equilibrium state is commonly encountered (e.g., Ross River Virus, Denholm et al., 2017).

From the point of view of wombat survival, the most important steady state is the mite-free case (9) in Section 3. In this case, the eigenvalue calculation yields the characteristic equation

$$\det(\mathbf{J} - \Lambda \mathbf{I}) = -[\Lambda^2 + (b + k + r)\Lambda + \lambda_R(b - \mu)] \times [\Lambda^3 + a_2\Lambda^2 + a_1\Lambda + a_0] = 0 \quad (19)$$

in which we have defined the constant coefficients

$$\begin{aligned} a_2 &= (m_E + \gamma) + (m_I + \mu_P) \\ a_1 &= (m_I + \mu_P)(m_E + \gamma) + \mu_P m_I - \frac{\beta(b - \mu)m_A \lambda_0}{b\lambda_R} \\ a_0 &= \mu_P m_I (m_E + \gamma) - (m_I + \gamma) \frac{\beta(b - \mu)m_A \lambda_0}{b\lambda_R}. \end{aligned} \quad (20)$$

The expression (19) is a quintic polynomial equation for the eigenvalue Λ , and so it has five roots. It consists of a quadratic polynomial multiplied by a cubic; the quadratic has two roots and the cubic has three. It is straightforward to calculate the two roots of the quadratic and to determine that, for $b > \mu$, their real parts are always negative. Thus the eigenmodes corresponding

to these two roots are always stable. Stability of the equilibrium point must therefore be determined by the three remaining roots of the cubic in (19). It is not, however, generally feasible to calculate the roots of the cubic directly in closed form, and so to determine whether or not their real parts are negative and the steady state therefore stable. We can use the Routh-Hurwitz criterion (e.g., see Murray, 1989) to determine a necessary condition for stability; this asserts that the roots of the cubic will all have negative real parts if the inequalities

$$a_2 > 0 \quad ; \quad a_0 > 0 \quad ; \quad a_2 a_1 > a_0 \quad (21)$$

all hold simultaneously. Thus the condition (21) must be satisfied for the steady state to be stable. The first condition in (21) is trivially true, and the second requirement $a_0 > 0$ leads to the *necessary* condition

$$\mu_P > \frac{\beta(m_I + \gamma)(b - \mu)m_A \lambda_0}{(m_E + \gamma)bm_I \lambda_R} \quad (22)$$

for stability of the mite-free equilibrium. We observe that the requirement (22) is not yet *sufficient* to guarantee stability, since the final inequality in (21) has not been satisfied. This is extremely difficult to do, and the algebra is overwhelming. In general, then, we only have the weaker (necessary) stability condition (22) as a *guide* to the stability of this important mite-free equilibrium point.

In the special case $\mu_E = \mu_I$, Beeton et al. (2019) were able to show that the last inequality in (21) is also satisfied, thus making their equivalent of (22) both a necessary and a sufficient condition for stability of the important mite-free steady state. A similar result is achieved here.

When $\mu_E = \mu_I$, the cubic in (19) can be written in the simpler form

$$\begin{aligned} & \Lambda^3 + a_2 \Lambda^2 + a_1 \Lambda + a_0 \\ & = [\Lambda + m_I + \gamma] \times \left[\Lambda^2 + (m_I + \mu_P)\Lambda + \mu_P m_I - \frac{\beta(b - \mu)m_A \lambda_0}{b\lambda_R} \right]. \end{aligned}$$

Now the three roots of this cubic can be identified at once. They are

$$\begin{aligned} \Lambda & = -(m_I + \gamma) \\ \Lambda & = -\frac{(m_I + \mu_P)}{2} \pm \sqrt{\left(\frac{m_I - \mu_P}{2}\right)^2 + \frac{\beta(b - \mu)m_A \lambda_0}{b\lambda_R}}, \end{aligned} \quad (23)$$

when $\mu_E = \mu_I$. The first of the eigenvalues in (23) is clearly negative and the next two are clearly real since their discriminant is positive. For these two to be negative, the square-root term must be smaller than the first term, which requires

$$\mu_P > \frac{\beta(b - \mu)m_A \lambda_0}{bm_I \lambda_R}. \quad (24)$$

This condition (24) is therefore both necessary and sufficient for the mite-free equilibrium to be stable, in the case $\mu_E = \mu_I$. The more general (necessary) condition (22) reduces to (24) for this case. This condition is directly related to (2.17) in Beeton et al. (2019)—replacing the shedding rate f from that result with $m_A = \mu + k + \alpha$ and μ_F with μ_P gives our result, suggesting that these two variables are equivalent in some sense.

The stability of the two endemic steady states (17) can be ascertained in the same way as above. The 5×5 Jacobian matrix of derivatives is calculated and evaluated at each of these two endemic states numerically to calculate the eigenvalues that determine stability. As a check, this purely numerical procedure was used for all four steady states, including the total extinction state and the mite-free equilibrium discussed above, and compared with the analytical results obtained here.

5 Presentation of Results and Discussion

We here present results produced by the system of equations (2)–(6) and interpreted by our analyses above and numerical simulation in the R programming language (R Core Team, 2018). We particularly focus on their biological significance and their relationship to the model of Beeton et al. (2019). We first summarise the broad characteristics our new model shares with the earlier one, then give a more detailed description of the differences. In particular, we examine the effect of parameters: those shared between the models, those unique to one of them, and the relationship of parameters between models (as indicated in the previous section above).

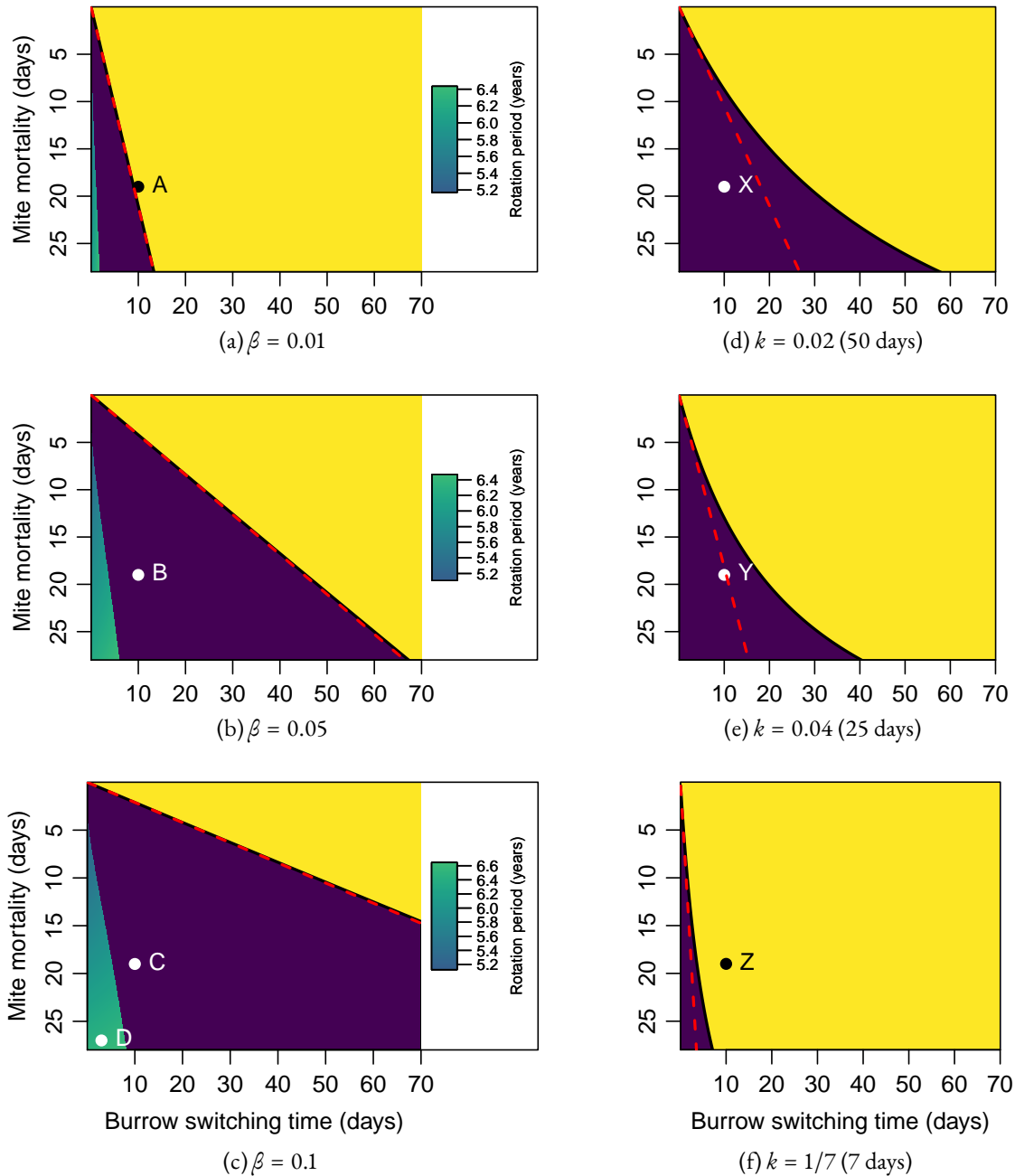


Figure 2: The stable states of the model at different expected values of burrow-switching time ($1/\alpha$) between 0 and 70 days, and expected mite life expectancy ($1/\mu_P$) between 0 and 28 days. For Figures 2a–c, no treatment is occurring ($k = 0$), but the burrow infection rate β is varied. For Figures 2d–f, β is set to 0.05 and the treatment rate k is varied. Purple represents the endemic (“plus sign”) and yellow the mite-free equilibria. Shades of blue represent a limit cycle around the endemic equilibrium, with period (in years) of small oscillations around the equilibrium determined by the shade: note that this differs from the limit cycle’s period of oscillation away from the boundary of the Hopf region. Red dashed lines represent the corresponding boundary between stability of endemic and mite-free equilibria from Beeton et al. (2019), with burrow-switching time α replaced with mite-shedding time f , and mite mortality μ_F replaced with μ_P . The labelled points A–D and X–Z represent points of interest that will be explored further. (For interpretation of the references to colour in this figure legend, the reader is referred to the web version of this article.)

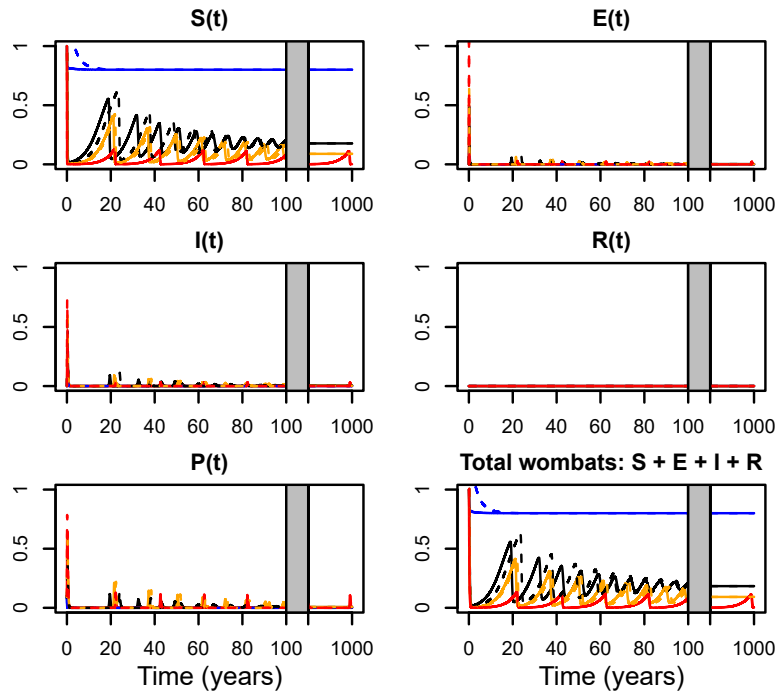


Figure 3: Time histories for the populations of the four sub-classes of wombat and for the fomite population. In addition, the total surviving wombat population is shown. Blue, black, orange, and red lines represent points A, B, C and D, respectively, from Figure 2. Solid lines represent the initial condition ($S = 1, F = 0.1$) and dotted lines the initial condition ($S = 2, F = 0.1$). Note that $R(t)$ is here identically zero in all cases due to the lack of treatment. (For interpretation of the references to colour in this figure legend, the reader is referred to the web version of this article.)

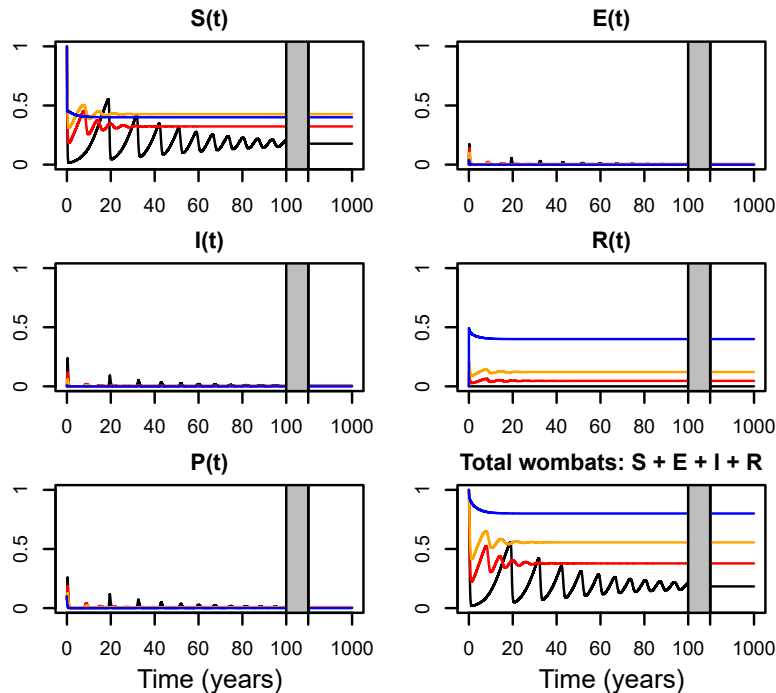


Figure 4: Time histories for the populations of the four sub-classes of wombat and for the fomite population. In addition, the total surviving wombat population is shown. Black, red, orange and blue lines represent points B, X, Y and Z, respectively, from Figure 2. The initial condition is ($S = 1, F = 0.1$) in all cases. Note that the black lines in Figures 3 and 4 represent the same trajectory (point B). (For interpretation of the references to colour in this figure legend, the reader is referred to the web version of this article.)

Following [Beeton et al. \(2019\)](#) and consistent with field measurements, we have set the wombat birth rate to be $b = 1/(3 \times 365)$ and their death rate as $\mu = 1/(15 \times 365)$. The additional death rates experienced by the exposed and infected wombats are taken to be $\mu_E = 1/60$ and $\mu_I = 1/60$, and the remaining rates in the model are chosen to be $r = 1/7$, $\alpha = 0.05$, $\beta = 0.1$ and $\gamma = 1/30$. We also experimented with scenarios where μ_E was increased or μ_I decreased (Appendices B and C, respectively), breaking the $\mu_E = \mu_I$ assumption: while these scenarios did qualitatively change the results, they did not change our conclusions so are not reported in the main text.

We combine the analytical results of the model derived in Section 4 and numerical simulation in Figure 2. The figure describes which state is stable at any given value for the pair of parameters α and μ_P , if any, for different scenarios involving values of β and k (see [Martin et al., 2019](#)). Figure 2 in [Beeton et al. \(2019\)](#) performs the same task but for the pair of parameters f and μ_P in their model; for the purposes of comparison, we have added in our Figure 2 a red dashed line denoting the boundary between stability of endemic and mite-free equilibria for those parameters and that model. As mentioned, the stability condition for the mite-free equilibrium (yellow in the figure) is the same in our model and the previous model, where $f = \mu + k + \alpha$ and $\mu_F = \mu_P$. As mortality (μ) is on a much slower time scale than either shedding rate or wombat movement (f and α), we see the results for that boundary where $f = \alpha$ and $\mu_F = \mu_P$ are near-identical when $k = 0$ (i.e., Figures 2a–c). As with that model, across the presented scenarios at most only a single state has all eigenvalues negative, thus being the stable state. For sufficiently slow wombat movement (i.e., low α , high wombat movement period) and high mite mortality rate (i.e., high μ_P and low life expectancy), the mite-free equilibrium (9) is stable; otherwise the “plus sign” endemic equilibrium (17) will generally be stable. Our results also match the previous model in that the mite-free equilibrium is stable at points A and Z and the endemic equilibrium is stable at points B , C , X and Y . In our model, the wombat population persists at these points at 0.2290, 0.1151, 0.4723 and 0.6947 respectively, where numbers are given as a proportion of the equilibrium mite-free abundance (i.e., $1 - \mu/b$). Where wombat movement between burrows is frequent and mite mortality is low, no equilibrium point will be stable—a Hopf bifurcation occurs and a limit cycle forms around the endemic equilibrium. This is the case for point D (burrow-switching time 3 days, mite life expectancy 27 days), and the population size oscillates between 0.0015 and 0.1234 in the long term.

Figures 3 and 4 show the evolution over time of the sub-populations of wombats and the states of the burrows under the different scenarios labelled in Figure 2. The former examines changing the burrow infection rate β (A , B and C) and exploring an example limit cycle (D). The latter examines changing the treatment rate k (B , X , Y and Z). Both figures examine an entirely susceptible population of wombats ($S = 1$, $E = I = R = 0$) along with 10% of burrows infected ($P = 0.1$), and Figure 3 additionally examines a population well above carrying capacity ($S = 2$) to test for potential additional effects due to resource-driven pressure. In the figures, it can be seen that the presence of mange causes the total population size to be held below the environmental carrying capacity. In Figure 4, it can further be seen that the population size returns to the environmental carrying capacity (if disease free) or close to it (if mites are not eradicated).

The trajectories follow a qualitatively similar path to those in the previous model: in Figure 3, the mange epidemic quickly dies out in Case A , but periodic epidemics continue in the other cases, slowly decreasing towards an eventual endemic state except in Case D , where periodic epidemics continue due to the limit cycle. For the original initial condition ($S = 1$), the minimum populations experienced during the simulations are 1, 0.0236, 0.0062 and 0.0010 for A , B , C and D , respectively. For $S = 2$, they are 1, 0.0118, 0.0055 and again 0.0010. As expected, increasing the infection rate rapidly increases the risk of extinction by Allee effects ([Murray, 1989](#)), and an overabundant population is likely to experience a more severe crash for moderate infection rates (B). However, as seen in Figure 4, even a small amount of treatment improves the situation significantly and avoids dangerously low population levels: the minima here are 0.2811, 0.5179 and 1 for X , Y and Z , respectively, with mange eradicated in Case Z .

The above results provide evidence that our model replicates the qualitative traits of that of [Beeton et al. \(2019\)](#) both during the transient phase and at equilibrium. However, there are interesting and important differences between the two models. In Figure 2, we see the similarity between α and f ends once we start increasing k , which is on the same time scale (unlike μ). As a result, eradicating mange becomes more difficult for our model compared to the previous one, especially where both burrow-switching rates and mite mortality are low. This is due to the spatially implicit nature of our model: even if wombats are not switching regularly between burrows, a persistent population of mites in some burrows will immediately infect any wombats that are born or revert from resistance in these burrows, allowing mange to remain endemic despite treatment. Our numerical simulations also pick up another important difference in equilibrium states: limit cycles can occur even at low infection rates (e.g., $\beta = 0.01$), whereas in the previous model a much higher infection rate (e.g., $\beta = 0.1$) was necessary to observe these. These limit cycles are particularly worrisome for wombats, as they experience repeated population crashes to potentially unsustainable levels, which are near-identical in both of our models.

There are also important differences in the transient behaviours of these models and the population sizes at equilibrium, as seen in Figures 3 and 4 of both papers. To summarise, for low infection rates, the population is less affected in our model, but population crashes are substantially more severe for intermediate infection rates (Case B ; the previous model experiences minima of only 0.0306 and 0.0162 for initial $S = 1$ and $S = 2$ respectively). The most obvious differences, however, are under treatment, with our model having substantially lower endemic equilibrium populations in both Cases X and Y (only 0.4723 and 0.6947 versus 0.5739 and 0.9616 respectively), consistent with the previous results.

6 Conclusions

The aim of this paper has been to compare a new spatially implicit model of mite transmission in wombats with a recent model by [Beeton et al. \(2019\)](#) that does not consider explicitly the role played by wombat burrows as a major contributor to the spread of mite-borne mange disease. Importantly, these two different models have nevertheless produced qualitatively similar conclusions; there is a steady state at which both species die out, a second steady state in which only the wombats survive, and a possible two further equilibria that describe endemic behaviour with mites and wombats in all the different stages of infection co-existing. These models are thus structurally robust, in the sense that different methods of describing the same overall biology yield the same types of behaviour. Both models are still likely to contain some incorrect assumptions that may result in inaccuracies when compared to field data; nevertheless, combining the two should provide more robust conclusions compared to using a single model and describe qualitative events that actually occur in the field. In particular, comparing the effects of management between the two models is important: we have shown that our new method requires a higher level of treatment to achieve mite eradication, and so using the previous method alone would likely produce overly optimistic results.

As for the simpler model ([Beeton et al., 2019](#)), the new model considered here also contains the important mite-free steady state, and achieving this would surely be the goal of any mite remediation programme (see also [Martin et al., 2019](#)). This would require that steady state to be stable, and an inequality (22) has been derived here that suggests conditions for achieving such stability. In accordance with common sense, it requires the natural death rate μ_p of the mites to be higher than a certain threshold, which itself can be lowered by increasing the treatment rate k or increasing the period of resistance (i.e., decreasing the reversion rate: see Figure A1, Appendix A). Again, this conclusion was also suggested by the simpler model of [Beeton et al. \(2019\)](#). In practice, we apply the treatment programme (rate k) by means of insecticide-laden flaps at the entrances of the wombat burrows, and the wombats must contact these each time they pass through the burrow entrances, although recent field research has suggested that the delivery success of treatment in the field is less reliable (as low as 1/3) ([Martin et al., 2019](#)). In addition, treatment and thus resistance is more likely to occur in pulses (see [Beeton et al., 2019](#)). In order to increase the death rate μ_p of the mites, it might also be necessary to supplement the treatment regime with other methods of treatment such as fumigation of targeted insect growth regulator chemicals to retard the growth of the mites ([Wardhaugh, 2005](#); [Chandler et al., 2011](#)).

Acknowledgements

The authors would like to thank Shane Richards and Geoff Hosack for their thoughtful comments.

Declarations of interest: none

Appendix A Decreased reversion rate

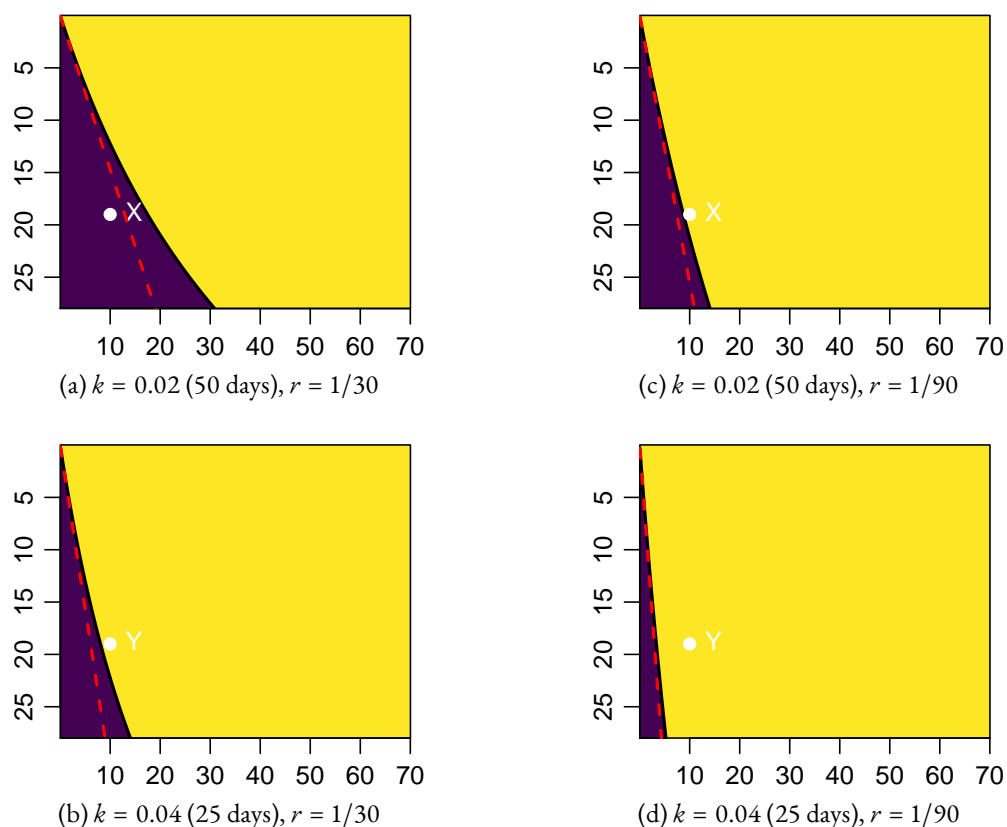


Figure A1: The stable states of the model at different expected values of burrow-switching time ($1/\alpha$) between 0 and 70 days, and expected mite life expectancy ($1/\mu_P$) between 0 and 28 days. For Figures A1a–b, the reversion rate is 30 days, with two levels of treatment ($k = 0.02$ and 0.04). For Figures A1c–d, the reversion rate is increased to 90 days. Purple represents the endemic (“plus sign”) and yellow the mite-free equilibria. Red dashed lines represent the corresponding boundary between stability of endemic and mite-free equilibria from [Beeton et al. \(2019\)](#), with burrow-switching time α replaced with mite-shedding time f , and mite mortality μ_F replaced with μ_P . The labelled points X and Y represent points of interest explained in the main text. (For interpretation of the references to colour in this figure legend, the reader is referred to the web version of this article.)

Appendix B Decreased μ_E

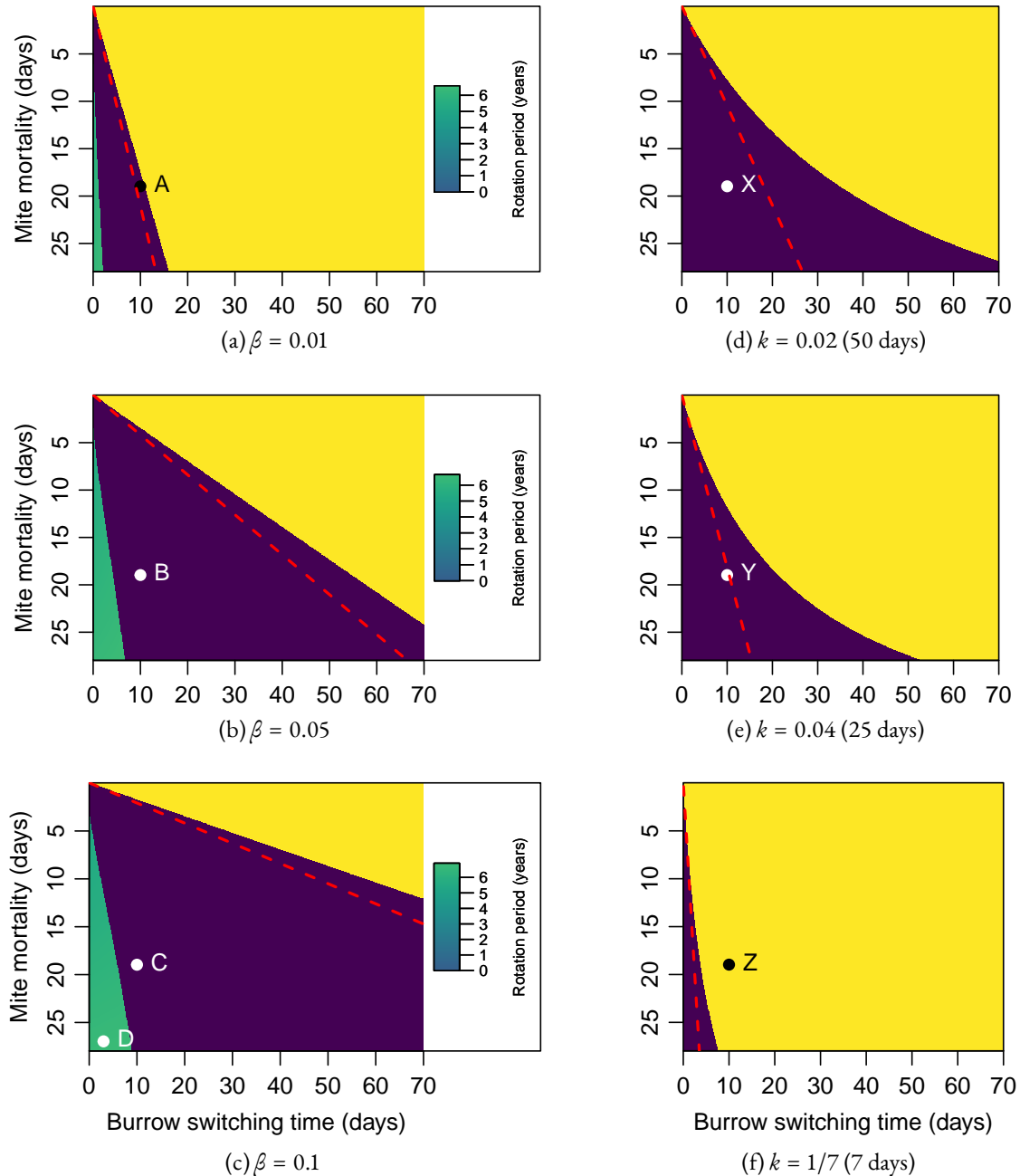


Figure A2: The stable states of the model at different expected values of burrow-switching time ($1/\alpha$) between 0 and 70 days, and expected mite life expectancy ($1/\mu_P$) between 0 and 28 days, as with Figure 2 but with μ_E reduced from $1/60$ to $1/120$. For Figures A2a–c, no treatment is occurring ($k = 0$), but the burrow infection rate β is varied. For Figures A2d–f, β is set to 0.05 and the treatment rate k is varied. Purple represents the endemic (“plus sign”) and yellow the mite-free equilibria. Shades of blue represent a limit cycle around the endemic equilibrium, with period (in years) of small oscillations around the equilibrium determined by the shade: note that this differs from the limit cycle’s period of oscillation away from the boundary of the Hopf region. Red dashed lines represent the corresponding boundary between stability of endemic and mite-free equilibria from Beeton et al. (2019), with burrow-switching time α replaced with mite-shedding time f , and mite mortality μ_F replaced with μ_P . The labelled points A–D and X–Z represent points of interest explained in the main text. (For interpretation of the references to colour in this figure legend, the reader is referred to the web version of this article.)

Appendix C Increased μ_I

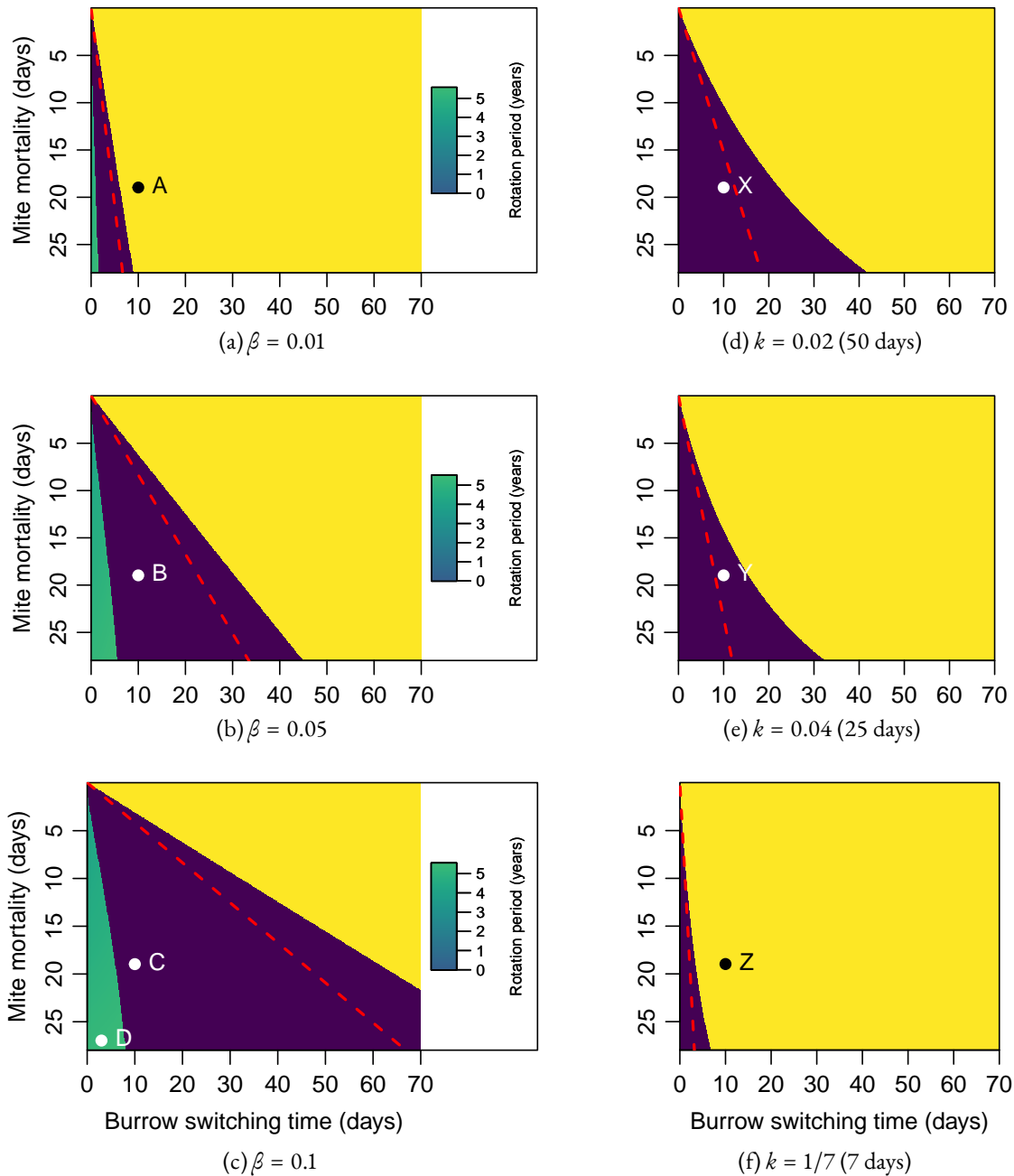


Figure A3: The stable states of the model at different expected values of burrow-switching time ($1/\alpha$) between 0 and 70 days, and expected mite life expectancy ($1/\mu_P$) between 0 and 28 days, as with Figure 2 but with μ_I increased from $1/60$ to $1/30$. For Figures A3a–c, no treatment is occurring ($k = 0$), but the burrow infection rate β is varied. For Figures A3d–f, β is set to 0.05 and the treatment rate k is varied. Purple represents the endemic (“plus sign”) and yellow the mite-free equilibria. Shades of blue represent a limit cycle around the endemic equilibrium, with period (in years) of small oscillations around the equilibrium determined by the shade: note that this differs from the limit cycle’s period of oscillation away from the boundary of the Hopf region. Red dashed lines represent the corresponding boundary between stability of endemic and mite-free equilibria from Beeton et al. (2019), with burrow-switching time α replaced with mite-shedding time f , and mite mortality μ_F replaced with μ_P . The labelled points A–D and X–Z represent points of interest explained in the main text. (For a colour version of this figure, refer to the web version of this article.)

References

- Arlan, L. G., and M. S. Morgan (2017). A review of *Sarcoptes scabiei*: past, present and future. *Parasites & Vectors* 10, 297. [3](#)
- Astorga, F., S. Carver, E. S. Almberg, G. R. Sousa, K. Wingfield, K. D. Niedringhaus, P. Van Wick, L. Rossi, Y. Xie, P. Cross, S. Angelone, C. Gortázar, and L. E. Escobar (2018) International meeting on sarcoptic mange in wildlife, June 2018, Blacksburg, Virginia, USA. *Parasites & Vectors* 11(449). [3](#)
- Beeton, N. J., S. Carver, and L. K. Forbes (2019). A model for the treatment of environmentally transmitted sarcoptic mange in bare-nosed wombats (*Vombatus ursinus*), *Journal of Theoretical Biology* 462, 466–474. <https://doi.org/10.1016/j.jtbi.2018.11.033>. [3](#), [4](#), [6](#), [7](#), [8](#), [9](#), [10](#), [12](#), [13](#), [14](#), [15](#), [16](#)
- Bornstein, S., T. Morner, and W. M. Samuel (2001). *Sarcoptes scabiei* and sarcoptic mange. In *Parasitic Diseases of Wild Mammals*, 2nd ed. Edited by Samuel, W. M., M. J. Pybus, and A. A. Kocan. Manson Publishing, London. [3](#)
- Chandler, D., A. S. Bailey, G. M. Tatchell, G. Davidson, J. Greaves, and W. P. Grant (2011). The development, regulation and use of biopesticides for integrated pest management. *Philosophical Transactions of the Royal Society B* 366(1573), 1987–1998. <https://doi.org/10.1098/rstb.2010.0390>. [13](#)
- Denholm, L., N. J. Beeton, L. K. Forbes, and S. Carver (2017). A model for the dynamics of Ross River Virus in the Australian environment. *Letters in Biomathematics* 4, 187–206. <https://doi.org/10.1080/23737867.2017.1359697>. [8](#)
- Devenish-Nelson, E. S., S. A. Richards, S. Harris, C. Soulsbury, and P. A. Stephens (2014). Demonstrating frequency-dependent transmission of sarcoptic mange in red foxes. *Biology Letters* 10(10), 20140524. <https://dx.doi.org/10.1098/rsbl.2014.0524>. [3](#)
- Fraser, T. A., M. Charleston, A. Martin, A. Polkinghorne, and S. Carver (2016). The emergence of sarcoptic mange in Australian wildlife: an unresolved debate. *Parasites & Vectors* 9, 316. [3](#), [4](#)
- Fraser, T. A., A. Martin, A. Polkinghorne, and S. Carver (2018). Comparative diagnostics reveals PCR assays on skin scrapings is the most reliable method to detect *Sarcoptes scabiei* infestations. *Veterinary Parasitology* 251, 119–124. [4](#)
- Hethcote, H. W. (2000). The Mathematics of Infectious Diseases. *SIAM Review* 42, 599–653. [7](#)
- Joseph, M. B., J. R. Mihaljevic, A. L. Arellano, J. G. Kueneman, D. L. Preston, P. C. Cross, and P. T. J. Johnson (2013). Taming wildlife disease: bridging the gap between science and management. *Journal of Applied Ecology* 50, 702–712. [3](#)
- Keeling, M. J. and P. Rohani (2008). *Modeling infectious diseases in humans and animals*. Princeton University Press, Princeton. [4](#)
- Lloyd-Smith, J. O., S. J. Schreiber, P. E. Kopp, and W. M. Getz (2005). Superspreading and the effect of individual variation on disease emergence. *Nature* 438, 355–359. [4](#)
- Lopes, C., T. Spataro, and R. Arditi (2010). Comparison of spatially implicit and explicit approaches to model plant infestation by insect pests. *Ecological Complexity* 7(1), 1–12. [4](#), [5](#)
- Martin, A. M., C. P. Burridge, J. Ingram, T. A. Fraser, and S. Carver (2018). Invasive pathogen drives host population collapse: Effects of a travelling wave of sarcoptic mange on bare-nosed wombats. *Journal of Applied Ecology* 55, 331–341. [4](#)
- Martin, A. M., S. A. Richards, T. A. Fraser, A. Polkinghorne, C. P. Burridge, and S. Carver (2019). Population-scale treatment informs solutions for control of environmentally transmitted wildlife disease. *Journal of Applied Ecology* 56(10), 2363–2375. <https://doi.org/10.1111/1365-2664.13467>. [4](#), [5](#), [12](#), [13](#)
- May, R. M. (1976). Simple mathematical models with very complicated dynamics. *Nature* 261, 459–467. [4](#)
- Mounsey, K. E., C. Bernigaud, O. Chosidow, and J. S. McCarthy (2016). Prospects for moxidectin as a new oral treatment for human scabies. *PLoS Neglected Tropical Diseases* 10, e0004389. [3](#)
- Murray, J. D. (1989). *Mathematical Biology*. Springer-Verlag, Berlin. [9](#), [12](#)
- Pence, D. B. and E. Ueckermann (2002). Sarcoptic mange in wildlife. *Revue Scientifique Et Technique De L'Office International Des Epizooties* 21, 385–398. [3](#)

- R Core Team (2018). *R: A language and environment for statistical computing*. R Foundation for Statistical Computing, Vienna, Austria. <https://www.R-project.org/>. 9
- Skerratt, L. F., D. Middleton, and I. Beveridge (1999). Distribution of life cycle stages of *Sarcoptes scabiei* var *wombati* and effects of severe mange on common wombats in Victoria. *Journal of Wildlife Diseases* 35(4), 633–646. 4
- Skerratt, L. F. (2005). *Sarcoptes scabiei*: an important exotic pathogen of wombats. *Microbiology Australia*, June 2005. 4
- Snäll, T., R. B. O’Hara, C. Ray, and S. K. Collinge (2008). Climate-driven spatial dynamics of plague among prairie dog colonies. *The American Naturalist* 171(2), 238–248. <https://doi.org/10.1086/525051>. 4
- Tompkins, D. M., S. Carver, M. E. Jones, M. Krkošek, and L. F. Skerratt (2015). Emerging infectious diseases of wildlife: a critical perspective. *Trends in Parasitology* 31, 149–159. 3
- Turing, A. M. (1952). The chemical basis of morphogenesis. *Philosophical Transactions of the Royal Society B* 237(641), 37–72. <http://doi.org/10.1098/rstb.1952.0012>. 4
- Wardhaugh, K. G. (2005). Insecticidal activity of Synthetic Pyrethroids, Organophosphates, Insect Growth Regulators and other Livestock Parasiticides: an Australian Perspective. *Environmental Toxicology and Chemistry* 24, 789–796. 13